Management and electric drive energy monitoring for the competition motorcycle IST MotoStudent- "TLMoto"

Gerardo Antonio de Lima Brito
Técnico Lisboa
Lisbon, Portugal
gerardo.antonio@tecnico.ulisboa.pt

***Abstract*— The aim of this thesis is to dimension, implement and test the electrical and propulsion system for the electric racing motorcycle prototype, TLM02e, developed by TLMoto team. TLM02e's electrical system is made up of an electric energy accumulator elected to be lithium batteries, a permanent magnet synchronous motor, motor controller and all of the additional electronics such as battery management system (BMS), electronic control unit (ECU), charging system etc.**

Given the competition regulations and hostile environment for electronics found in any electric vehicle, this design had to be carefully thought to conform to the competition constraints as well as being reliable, safe, efficient and resistant to vibrations, temperature, liquid and electromagnetic interference (EMI). Taking into account monetary limits and emphasizing more reliability than complexity some ideas such as gearbox or supercapacitors were eliminated from consideration.

At the end the system was tested in a test bench and is expected to be mounted in TLMoto's TLM02e electric motorcycle prototype hopefully achieving good results in the MotoStudent competition.

Keywords: Automatic measurement system, Battery management system, Electric vehicle, Electric motorcycle, Lithium battery, MotoStudent.

I. Introduction

A. Project Scope and Objectives

The MotoStudent competition [1] is a challenge between teams from different universities in the world. The aim of this competition is to design and develop a motorcycle that will be evaluated statically and dynamically in the final event on Motorland facilities in Aragon, being the static tests called for "MS1 phase" and the dynamic tests "MS2 phase" [2].

This work is mainly focused in applying electrical engineering knowledge in order to be competitive in MS2 phase always in accordance with the technical regulations, economical limits and reliability aspects.

Table I - MS2 phase scoring [2]

Class	Session	Test	Score
Dynamic tests	Track tests	1. -Brake test	60
		2. -Gymkhana	100
		3. -Best acceleration	60
		4.-Mechanical test	30
Race	Box test	5.-Maximun speed at ST	30
	Free practices	6.-Pole position	40
	Timed practices	7.-Fastest lap during race	30
	Race	8.-Race position	150
		Total	**500**

B. State of the art

Since this is the first time that TLMoto is building an electric motorcycle, there is not much information available from previous teams or previous prototypes that could serve as guidance in technical aspects. In this way, it was necessary to dimension the electrical system with caution and add some safety margin in the design with respect to security and completing the dynamic tests.

For a state of the art guidance Play and Drive's [3] electric motorcycle presented in fig. 1 was used.

Fig. 1. Play and Drive's MotoStudent electric [3]

Play and Drive is a company that build electric racing vehicles and has a technical partnership with MotoStudent organization. Their MotoStudent electric motorcycle uses the same motor as the one provided by the organization to all teams. This motorcycle was useful source of figures of merit, such as a battery capacity, weight or even starting point for gear ratio calculation. It was also possible to refer to commercial electric motorcycles of comparable power and weight.

C. System definition

The typical propulsion system of an electric vehicle is typically made by the energy accumulator, the electric motor and the power converter which regulates the power flow between the motor and accumulator.

Since the motor is mandatorily the same for all the teams and it cannot be modified only the energy storage unit, the power converter and the rest of the electronics could be chosen.

Table II - Provided electric motor specifications [2]

MOTOR PERM PMS 150 - RLS	
Type	AFPM Motor
Rated Power	13kW
Cooling	Air
Max speed	6000rpm (without field weakening)
Rated voltage	96VDC
Rated current	153A
Peak stall current	550A
Rated torque	20.7N.m
Peak stall torque	71N.m
Motor constant, Ke	0.0087V/rpm
Motor weight	22.3kg
Encoder	RLS-RMB29AC01SS1, analogic sin-cosin, power +5 V (independent GND)
Temperature sensor	KTY-84

Thanks to the MotoStudent organization, TLMoto had the chance to acquire a bundle of additional components specially prepared for the competition. These components included a motor controller, isolated DCDC (DC to DC) converter, battery charger and power contactors.

Considering all the main components initially purchased, a summary of the situation is presented in fig. 2.

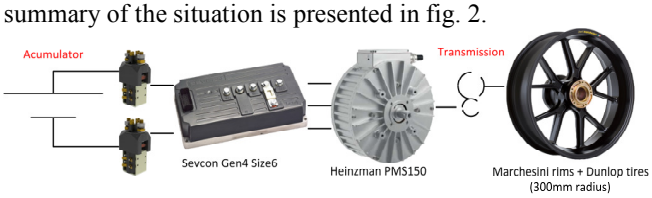

Fig. 2. Propulsion system diagram

II. Propulsion System Dimensioning and Optimization

A. Physical modeling

The main components of the electric propulsion missing dimensioning are the type and capacity of the energy accumulator and the gear ratio between the motor and the wheels chosen to be fixed. A Simulink block based model was made in order to help on these calculations but also the study of regenerative braking and other concerns.

1) Dynamics

From fig. 3, where all major forces acting on the motorcycle are represented, (1) can be written.

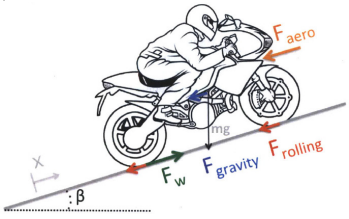

Fig. 3. System of forces applied to the electric motorcycle [4]

$$\sum F = m\ddot{x} = F_w - F_{aero} - F_{rolling} - F_{gravity} \qquad (1)$$

Here $m\ddot{x}$ is the resultant of the forces applied to the vehicle, F_w the propulsion or braking force, F_{aero} the aerodynamic frictional force, $F_{rolling}$ rolling frictional force, $F_{gravity}$ the component of the force due to the track slope. From reference [4] equation (1) can be developed as follows:

$$\dot{x} = \frac{1}{m}\int \left[F_w - \frac{1}{2}\rho C_d A(\dot{x}+w)^2 - mgC_{rr}Cos\beta - mgSin\beta\right] \qquad (2)$$

Where m is the motorcycle plus pilot mass, ρ the air density, C_dA the drag area, g gravity acceleration, C_{rr} rolling resistance coefficient, β is the track angle and the wind speed w is considered to be zero. The value of the constants was based on comparison with other motorcycles and estimation.

The Simulink "Dynamics" block was based in the implementation of (2), having as input the traction force, brake force and track slope and as output the speed and position of the motorcycle.

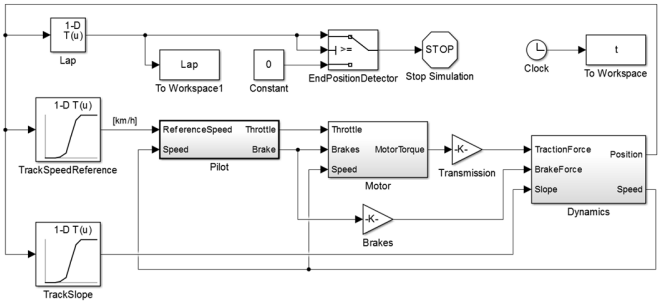

Fig. 4. Top diagram of the model

Beyond the dynamics block there is also the motor block, pilot block, the track slope table which gives slope as a function of position and the speed reference table. The speed reference table limits speed on certain sections of the track were the motorcycle cornering capability limits its speed [5]. It was obtained by discussion between team members and by viewing videos of similar race geometry motorcycles in the internet.

Through this last table and through a proportional controller the acceleration and braking behavior of the pilot is obtained as function of motorcycle position on track.

2) Motor

For the simulation of the motor its torque-speed characteristic and its efficiency map [6] is used.

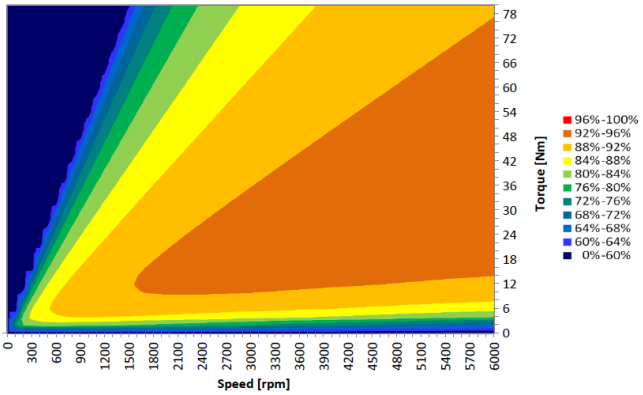

Fig. 5. Efficiency map provided by the manufacturer [6]

A small matlab script was created to pass the efficiency map image in .png format to an array in matlab workspace that was later used in the model in the form of lockup table for the

efficiency as a function of motor rotational speed and the torque working point.

Because of the thermal constant of the motor, the torque available from the motor is a curve of choice lying between the maximum peak torque and the nominal torque defined by the manufacturer for continuous operation. As this choice is dependent on the motor thermal characteristics and therefore difficult and complex to model, a plausible curve that will need further validation is chosen.

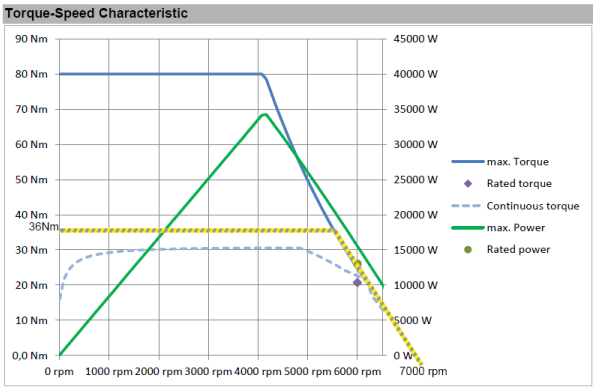

Fig. 6. Curve chosen as torque limit [6]

The chosen curve is the maximum peak torque limited to 36Nm at all rotations, in practice this can be done limiting the current supplied by the motor controller.

3) Brakes

The braking force was modeled as a constant force modulated by the pilot's command. The choice of this constant force to be modulated was based on the data of commercial motorcycles in which a deceleration of 1G was a common value for a wide range of motorcycles [7].

4) Transmission

The transition is a fixed gear ratio, here it is defined by division of the motor sprocket by the rear wheel sprocket.

To get the traction force from the motor torque (3) is used.

$$F_w = MTorque\left(\frac{1}{WheelRadius \times GearRatio}\right) \quad (3)$$

B. Gear ratio optimization

For the choice of an ideal gear ratio, the simulation command is inserted within a conditional loop in matlab to sweep a range of feasible transmission ratios and obtain the performance results for each of them, making therefore easy to choose the gear ratio that brings the best performance.

Two cases are considered, one for the acceleration test and another for the final race. The objective function to minimize in the case of the acceleration test was the time to complete a 150m straight in full throttle acceleration and in the case of the final race the time to complete one lap, remembering that it is allowed to change the gear ratio between dynamic tests.

After the optimization cycles the obtained best gear to use in the acceleration test is approximately 0.15, with a corresponding time to complete the 150m straight of 7.28s.

For the final race, the obtained optimal gear ratio was 0.2 with a respective lap time of 2:46 minutes.

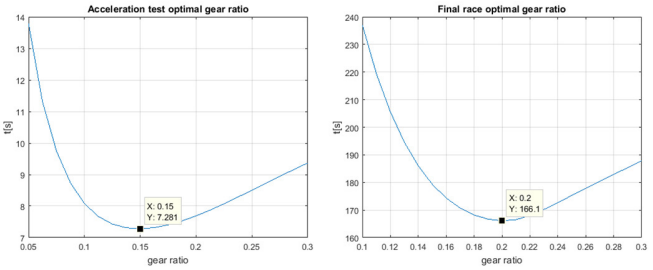

Fig. 7. Acceleration test and final race optimal gear ratios

C. Energy estimated for the accumulator

The dynamic test that will request more energy is by far the final race. Using the previously obtained sprocket ratio of 0.2 the simulation result provided us a value of approximately 4.28kWh.

As seen before the greatest uncertainties in this model relate to pilot behavior and the maximum average power it is possible to use from the motor without damaging its winding, so the solution was to opt for a margin of energy for the accumulator. This simulation did not counted with regenerative braking.

D. Regenerative braking

The regenerative braking power is limited by the current the accumulator can recover during the process when the motor plus motor controller acts as a generator. As will be seen in next chapters, in the implementation this maximum inverse current will be 128A and therefore the corresponding maximum braking torque is the multiplication of this current times the torque constant of the motor.

Simulating again the entire race with regenerative braking the total electrical energy consumed is 4.12kWh versus the previous 4.28kWh.

Knowing that no big energy recoveries are obtained, at least for the final race regenerative braking is not considered an implementation of priority, but its utility in braking power for the brake test must be tested when the motorcycle is built.

III. Accumulator

A. Types of energy accumulators

The most important figures of merit for this application are energy density (Wh/kg) and power density (W/kg).

Following the technical regulations, any type of accumulator may be use as energy storage system, except for thermal batteries and fuel cells.

For technical reasons options like flywheels or other kinds of non-conventional technologies are abandoned since these would have to be dimensioned and fabricated from scratch [8]. After considering various options, only supercapacitors and electrochemical batteries remained. Electrochemical batteries are chosen since supercapacitors alone would yield an unfeasible heavy accumulator.

Among electrochemical batteries, the best option when it comes to energy and power density is the lithium battery technology [9]. Within this technology, there are several variants, distinguished especially by the chemical compound used in the cell's cathode, being the main ones found on the market:

a) Lithium Cobalt Oxide (LCO).

b) Lithium Iron Phosphate (LFP).
c) Lithium Nickel Manganese Cobalt Oxide (NMC).

B. *Commercial lithium batteries*

After an intensive search for the lithium batteries with the best figures of merit plus the best value (Wh/eur), both as unitary cells or as a battery pack, a final list of the best candidates was obtained.

The energy calculations for Wh/kg and Wh/eur during this stage was simply the multiplication of the charge capacity by the single cell nominal voltage divided by the weight or price respectively. The problem of this approach is that it does not make accurate distinction because their manufacturer details are obtained at very different conditions. For example, some cell manufacturers claimed their capacity for a 20C rating while other did it only for 1C. This would yield an unfair comparison since typically for the same cell the higher the discharge rate the lower the supplied energy.

C. *Automated lithium cell tester*

The solution was then to build the embedded system shown in fig. 8.

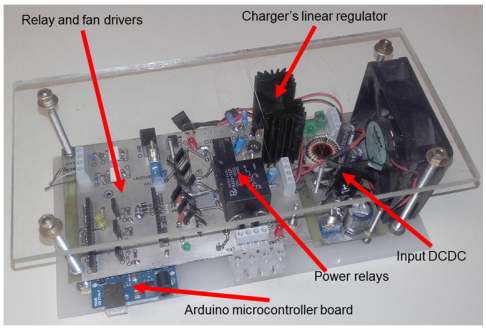

Fig. 8. Automated lithium cell tester main components

The function of this system was to automate the charging and discharging of cells acquiring the voltage and current of both operations so that these data could be used to analyze battery energy capacity.

This system works in conjunction with an Arduino microcontroller, has a 5A charger, possibility of connecting an external load resistor of choice and a set of relays that perform the various connections of the three main states of operation, which are charge, discharge and rest.

The Arduino has the task of data acquisition, communication with computer via USB, control signals for relays and some optional peripherals like fans, audible alarm, etc. The communication with the computer is used to interface with matlab where a script does most of the processing.

D. *Lithium cell tests*

The lithium cell discharges were made at the same C rating that was expected on the motorcycle (3C) and then at a higher rating (5C).

After many hours of data acquisition, several curves for various cells and discharge ratings were obtained. Only some of the obtained curves were selected namely the ones obtained in more ideal and similar conditions.

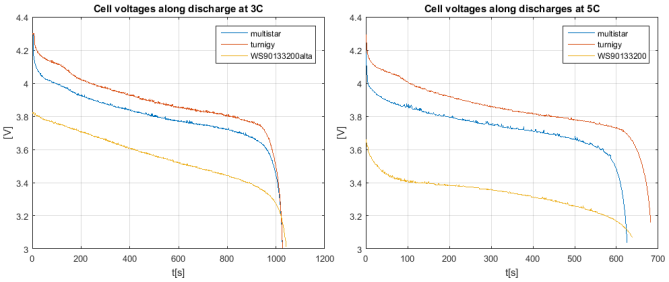

Fig. 9. Cell voltages along discharge at 3C and 5C

For data analysis, the product of voltage times current was integrated over time to obtain the energy capacity.

With the new capacity values, the figures of merit were recalculated and the best cell selected. The best cell obtained was of the same king of the ones used in aerial drones and sold in the form of a 4S2P battery pack.

Fig. 10. 16Ah 4S2P multistar battery pack (cover removed on right photo)

E. *Battery pack configuration*

Given the maximum permitted battery voltage of 110V, it was decided to put 27 cells in series and charge each one to 4.07V. The main reason for having 27 series cells and not 26 was the advantage of having three electrically equal battery stacks and BMS.

Calculating the number of parallel cells, a 3P setup would yield a 4.2kWh battery pack, even though this was very close to the simulated energy requirement, as safety margin a 4P setup was used, yielding 5.6kWh pack at the cost of more 8kg of weight.

For the parallel strings there are several options regarding their interconnections as is illustrated in fig. 11. Option (b) is adopted since this approach saves battery management system (BMS) boards but care must be taken about the currents that cross these parallel interconnections, in terms of the current carrying capabilities of the conductors and cell voltage reading errors on the BMS.

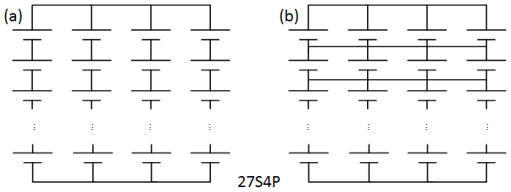

Fig. 11. Parallel interconnection possibilities

To get an idea of how parallel cells behave when it comes to current distribution, various experiences were held in order to empirically get the peak current of these parallel interconnections.

IV. Motor, Controller and HVS

The two main systems of the motorcycle defined by the regulations are the high voltage system (HVS) and the grounded low voltage system (GLVS)

The high voltage system is made by all components with a voltage exceeding 40VDC. The GLVS instead has a voltage below 40VDC which must be galvanically isolated from HVS, this isolation requirements are explained through various spatial and constructive constraints in the competition regulations.

A. Motor controller

The motor controller implements itself many functions [10] including the power converter, permanent magnet synchronous motor (PMSM) control, as well as various additional functions as pre-charge of the converter input capacitor, direct inputs for throttle, programming of parameters, connection to a controller area network (CAN), etc.

The way the motor controller is enabled is related to an important aspect of the regulation namely the compulsory "disconnection circuit".

B. Disconnection system

The disconnection system is a safety measure that consists in disconnecting the main contactors between the batteries and the motor controller if any abnormality is detected.

In the designed system, the motor controller itself controls the main contactors, so in order to disconnect them the controller must be disabled through its key switch input. This electrical pin is in series with various switches and with the solid-state relays (SSRs) in the electronic control unit (ECU) so that a chain of conditions must be met to enable the motor controller:

1) The low voltage power must be turned on (GLVS), enabling 12V to come out of the isolated DCDC converter.
2) Traction button must be activated by the pilot.
3) Safety buttons (SERVICE) must remain in their usual normally ON position.
4) The IMD (insulating monitoring device) should not detect any insulation problem between HVS and GLVS.
5) There should be no problems with the battery such as excessive temperatures or operation outside the rated voltage range, this being detected by the BMS.

Conditions 2 and 3 are controlled by switches connected in series with the key switch input while conditions 1,4 and 5 are controlled by the ECU through the SSRs.

C. Charging System

Despite slight differences in ideal charging of different batteries chemistries, all are based on a constant current regime followed by a constant voltage until current is zero or in practice negligibly small.

The Lithium cells have manufacturing deviations and therefore there are usually capacity imbalances between cells in series and parallel. The imbalance is a situation to avoid as it forbids us to use the maximum available capacity of the full battery pack. For this reason, is necessary to find a method of balancing the cells.

The main two types of methods are the active and passive methods. The active method consists in transferring charge from the most charged cells to the less charged, this is the most energy efficient method in comparison to the passive method which is limited to discharge the most charged cells until all cell voltages are equalized.

Despite the energetic efficiency advantage, the active balancing is more complex and since the main race is relatively short in time, there is no time to make a useful balancing during the race with a practical active balancing system. For these reasons, a simple passive balancing is used.

The passive balance of the cells is performed during the charge, so the ideal balance power is a function of the time available for charging batteries during the competition and the quantity of imbalance that they suffer in a full discharge/charge cycle.

Knowing that at least 1 hour and 40 minutes is available for charging, only the amount of imbalance that the cells undergo remains to be estimated. For this a experiment was performed in which cells starting with the same voltage at their terminals were fully discharged and subsequently recharged with a C rating close to the one expected in the motorcycle. In the end of the experiment, the difference in capacity between the least and most charged cell is estimated. Then the cell voltage were to start balancing is chosen and knowing the time difference, the balancing load power is calculated and extrapolated to the motorcycle case. The obtained balancing power was approximately 32W for each group of parallel cells.

Since in the worst case the total balancing power would round 822W and since this could bring temperature problems on the battery container, the balancing load is installed outside the motorcycle.

V. Electronics and GLVS

A. Insulation monitoring device (IMD)

In fig. 12 the typical voltage potentials found on an electrical vehicle [11] is presented. Mainly there are the high voltage circuits and the separated earthing structure which should be connected to the motorcycle chassis and any other metallic part exposed to the pilot.

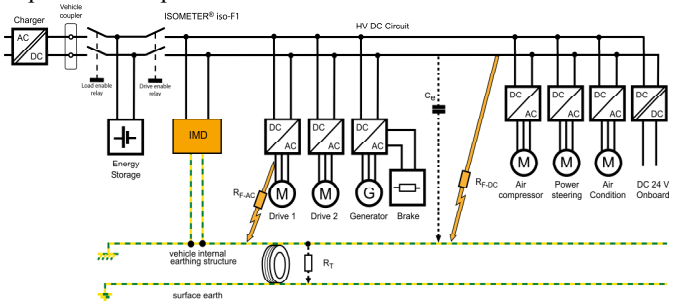

Fig. 12. IMD typical application on an electric vehicle [11]

The main function of the IMD which is compulsory and provided to all teams by the organization is to ensure that the impedance between the high voltage circuit and the low voltage circuit is always above a certain value so there is no danger to the pilot in terms of exposed high voltage. In case the impedance goes below a specified value it adverts the ECU through an electrical signal and them the ECU triggers the disconnection circuit as already explained.

B. *Electronic Control Unit (ECU)*

In automotive electronics, Electronic Control Unit (ECU) is a generic term for any embedded system, which controls one or more of the electrical system and subsystems in a transport vehicle.

1) *ECU main functions*

In this application, the ECU performs the essential task of implementing part of the disconnection circuit by controlling the SSRs.

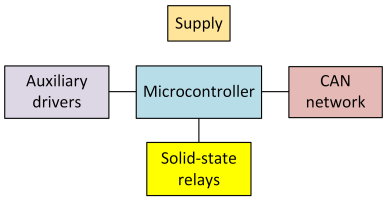

Fig. 13. Main functions of the ECU printed circuit board (PCB)

For the implementation of the ECU the STM32F446 microcontroller is chosen, this microcontroller was also used on the BMS boards.

Since there was already an isolated DCDC converter supplying all the motorcycle GLVS electronics and this board did not had to be isolated from the main ground (chassis), simple linear regulators were used to convert the 12V GLVS voltage to 5V and 3.3V, booth needed by the ECU components.

Because of the motor controller, the CAN ground reference is at the same potential of the battery negative terminal. For this reason and since direct connection to the CAN electrical signals would compromise the electrical isolation between the HVS and GLVS an isolated CAN transceiver was a necessity. The chosen chip was the ADM3053 transceiver.

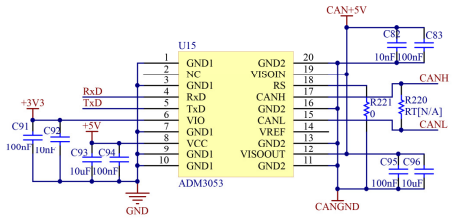

Fig. 14. CAN transceiver schematic

The chosen SSRs (IXYS CPC1927) are capable of switching DC loads, with a current carrying capability above the motor controller's key switch peak input current and comes in a very compact through-hole encapsulation. This made possible to incorporate them directly in the PCB, avoiding more external components, simplifying wire harness and enhancing reliability.

An auxiliary fan driver was added just in case fans had to be used to cool down the battery container or any other part of the motorcycle.

Maximum care was taken in designing a reliable board by using bypass capacitor were necessary, being concerned about power dissipation of some devices, adding freewheeling diodes on inductive load drivers and fuses plus transient voltage suppressor in various inputs/outputs such as the board input supply.

Most of the chosen components are mainly surface mount device (SMD) technology, as it is the most current nowadays and therefore have lower prices and a wider variety.

2) *Layout*

For costs reasons, space available and mainly electromagnetic compatibility (EMC) considerations the size of the board was kept at the minimum possible.

As already explained attention was taken to heat dissipation of some components for example the input linear regulators, these required thermal coper planes in order to help dissipate heat. Other concerns were related to noise were for example the reset trace was kept away from other "fast" digital signals in order to avoid accidental resets due to electromagnetic coupling.

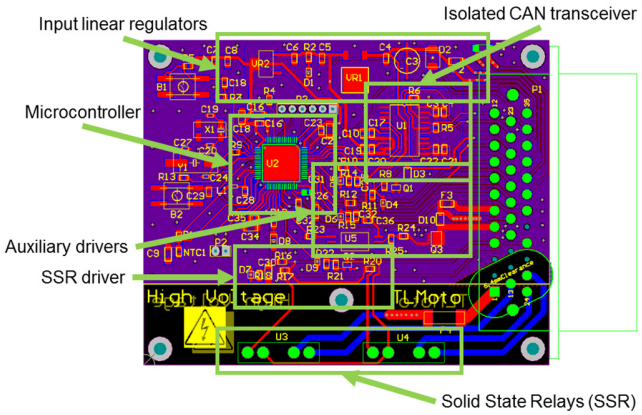

Fig. 15. ECU main components

Next to the SSRs were the high voltage traces are located, the coper planes were removed both on top and bottom and the HVS circuits were kept at a minimum clearance of 6.4 millimeters from the GLVS as explained in the regulations.

C. *Battery management system (BMS)*

In this application, a modular BMS architecture was used, having three stacks of 9S4P cells and each one with its own BMS PCB.

1) *BMS main functions*

The main parts/functions of the BMS are resumed in fig. 16.

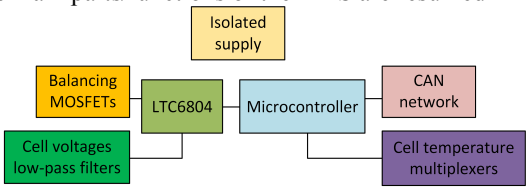

Fig. 16. Main functions of the BMS PCB

The power supply for the BMS had to be isolated since each BMS ground is at different voltage potentials namely each BMS is connected to its corresponding most negative cell terminal.

The solution was to use an integrated isolated DCDC converter. The chosen model was the TEL5-1211 capable of delivering 1A with an output voltage of 5V. On the second regulation stage, simple 3.3V linear regulator chip was used.

For the electronic construction of the BMS, besides the STM32F446 microcontroller an auxiliary integrated circuit (IC) was used. The chosen IC was the LTC6804 [12] since it

presented good characteristics, was available on the market and was used in other well-documented projects [13]. The LTC6804 eases the task of cell voltage reading and balancing metal–oxide–semiconductor field-effect transistors (MOSFETs) control. The typical application diagram of the respective datasheet is shown in fig. 17 here the p-channel MOSFETs, the balance resistors and low pass filter are exemplified for 12 battery cells in series.

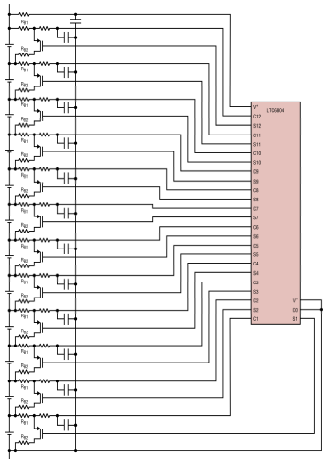

Fig. 17. LTC6804's datasheet application example [12]

In the motorcycle implementation only 9 cells need to be monitored by each BMS, for this reason and following the datasheet recommendation the cell number 12,11 and 6 were shorted for a zero potential cell reading. A fuse was added on each input since it was not only important for short circuit protection but also compulsory by the regulations.

For the cell temperature readings analog multiplexers were added since the number of analog inputs on the microcontroller was not enough.

2) Layout

For the same reasons of the ECU this PCB was kept at its minimum possible size. In fig. 18 the layout and component placement is illustrated on top and bottom of the board layout. Even the MOSFETs had a very low ON resistance, top and bottom coper planes were used in order to avoid an external heat sink and therefore keep the BMS PCB thin and light.

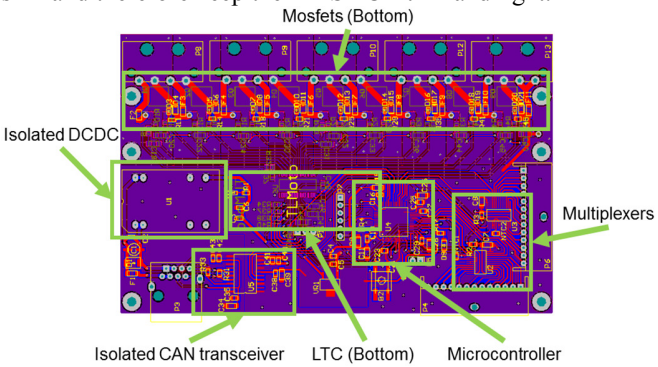

Fig. 18. BMS main components

VI. Implementation and Test

A. Electronic printed circuit boards

After the design and layout of the printed circuit boards prototypes were fabricated for each one of them with the traditional toner transfer method. The objective of the first prototypes was to test the main functions before passing to the final implementation.

1) ECU final implementation

Even that no big adjustments were necessary between the first prototype and the final version it was an important step since in this way TLMoto electrical team could start programing earlier.

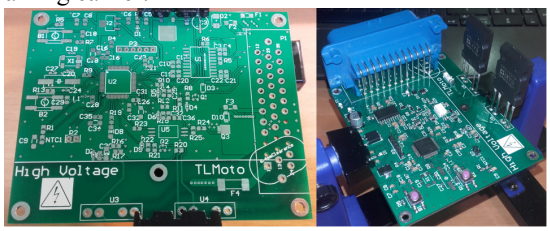

Fig. 19. ECU final implementation

2) BMS implementation

For the BMS there were three prototype iterations. The first consisted in a breakout board for the LTC6804 chip and the last two consisted in the entire BMS board.

The breakout board consisted on all of the final BMS bottom circuits closely related to the LTC chip. The main objective of this board was to start testing and learning some of its functions independently of the used microcontroller.

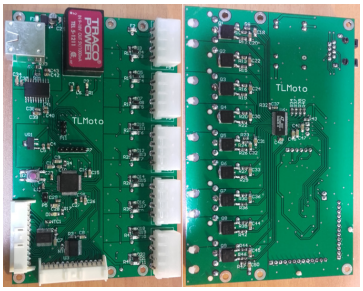

Fig. 20. BMS final implementation

B. Battery pack construction

After the removal of the original package (see fig. 10), balancing and power connectors were soldered to the terminals of each cell. Then the balancing and BMS wires harness was built. All the wires used in the battery pack had silicone insulation which is high temperature resistant (+-180ºC versus traditional 105ºC) and non-flammable making these compliant with MotoStudent regulations. The current rating also played an important role in the choice of wire conductor area in which the maximum current the blue wires had to withstand was the balancing current of circa 7.5A and circa 15A for the grey wires of the cells parallel interconnections.

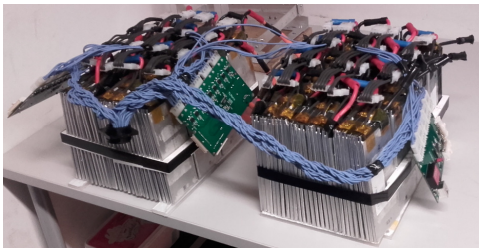

Fig. 21. Battery pack ready to have temperature sensors installed

The temperature sensors used are based on negative temperature coefficient (NTC) resistors with SMD encapsulation (NCP18XH103F03RB) manually soldered to wires connecting to BMS multiplexers. To avoid short circuits and damages in the cells these sensors were covered in epoxy glue near the NTC zone and latter with electrical tape for extra safety.

C. Test bench

The main objectives of test bench was to test the temperature of the motor, motor controller and batteries, monitoring the energy consumed/obtaining the total energy contained in the final battery pack, test the quality of the power connections and finally test the automatic shutdown system.

In order to meet the objectives the experiment shown in fig. 22 was prepared. This experiment consisted of a test bench in which the motor of the motorcycle was coupled through a transmission chain to a generator with a resistive load.

Due to the maximum power of the generator, the dissipated power was limited to 10kW.

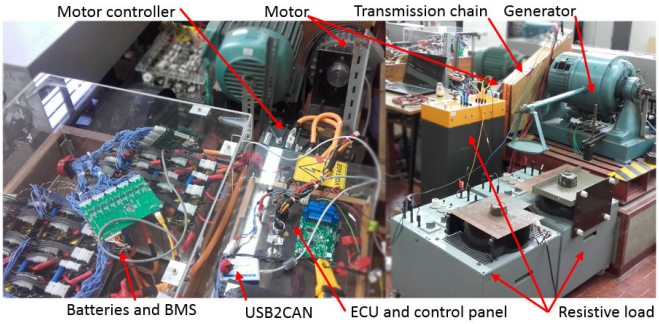

Fig. 22. Test bench (other components like the IMD were later added)

For the choice of the motor-generator gear ratio, the generator data was taken into account. This generator consisted in a DC machine with separated excitation field. The transmission was made with a motorcycle chain in which the ratio was chosen so both, the motor and the generator could rotate near their rated speeds helping on the power transfer.

1) Choice and monitoring of temperature limits

The chosen temperature range for the cells was -20°C to 60°C since this was the most common interval found in the bibliography [9].

The manufacturer preconfigures the maximum temperature of the motor controller to 75ºC. At this temperature it starts to limit the power supplied to the motor. The controller also has the ability to limit this power when the motor temperature exceeds the configured value.

In order to know the motor temperature, the controller uses two methods: direct measurement through a sensor built into the motor windings and through an estimation method. Both methods are already configured by the vendor of the equipment, leaving us the choice of the limit to impose.

Taking into account several constraints listed in the motor documentation a maximum motor temperature of 125ºC was chosen.

In order to try to match the conditions that will be found in the motorcycle or that are required by the motor manufacturer, several fans of various types were used for the motor controller, motor and battery.

2) Automatic measurement system

Thanks to the built electronics and motor controller's CAN network compatibility all the necessary data was available from the test bench and acquired with a USB-to-CAN device. The entire acquisition scheme is shown in fig. 23. Here the USB-to-CAN device and its software "IXXAT MiniMon" saves the CAN data to a *.cvs file type which is then opened via a purpose written matlab script. This enabled to view graphics of the variables during the course of the experiments.

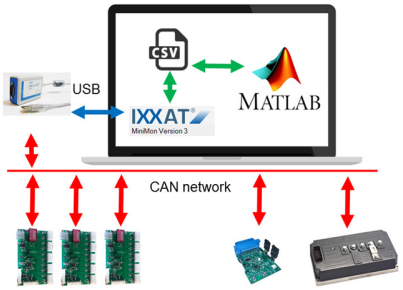

Fig. 23. Test bench data acquisition and monitoring scheme

The acquired data of interest is listed in table iii.

Table III - Data acquired from the CAN network

ID (hex)	Source	Comments
B	BMS1	Voltages from cells monitored by BMS1
C	BMS2	Voltages from cells monitored by BMS2
D	BMS3	Voltages from cells monitored by BMS3
15	BMS1	Temperatures from cells monitored by BMS1
16	BMS2	Temperatures from cells monitored by BMS2
17	BMS3	Temperatures from cells monitored by BMS3
222	Controller TPDO1	CAN message containing the heatsink temperature, motor RPM.
223	Controller TPDO2	CAN messages containing the variables: motor temperature, torque, capacitor voltage, battery current.
283	Controller TPDO5	CAN messages containing the variables: throttle input voltage.

3) Full load test

During this experiment, adjustments were made along the way in order to keep the power provided to the generator close to its nominal.

None of the temperatures was overpassed and it was concluded that if conditions such as similar ambient temperature are met more power than this will be available from the motor.

Finally, the electrical power was integrated in order to obtain the battery capacity in Wh. The 5.5kWh obtained energy was very close to the calculated energy capacity for the pack in section 3.

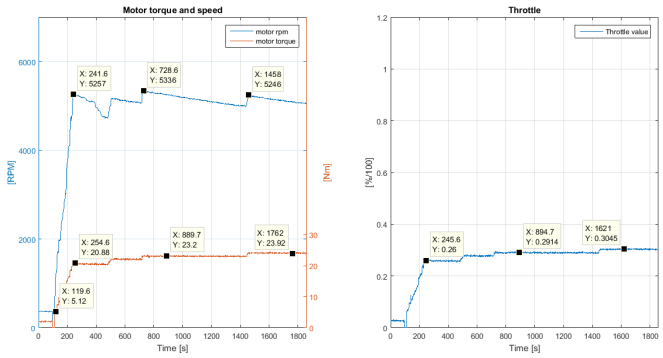

Fig. 24. Motor mechanical variables

Immediately after the automatic shutdown, a thermal imager instrument was used to confirm the temperatures read in several parts of the test bench.

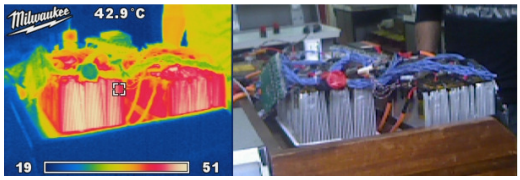

Fig. 25. Battery cells thermal image

The thermal imager was also useful to look for hot spots in the assembly that could show bad electrical contact or bad current distribution between parallel conductors. No problems were detected.

4) Electrical waveforms

In order to confirm which power cables were more prone to emit electromagnetic noise, the current and voltage waveforms at nominal load were acquired at the battery terminals and at one phase of the motor.

Thanks to the input capacitor of the motor controller, the input current ripple is low drastically reducing the noise emission in the connections between the controller and batteries and also between cells. The same is not true for the motor connections where a pulse width modulation (PWM) voltage and a sinusoidal current both with reasonable magnitude and/or frequency was observed. Fortunately, it is anticipated that in the motorcycle the connections between controller and motor will be relatively short and far away from the rest of the low power electronics.

5) Disconnection tests

During the various tests performed, it was confirmed that the automatic shutdown of the BMS operated for both temperature and voltage limits.

It was also confirmed that the IMD disconnects the contactors (by the ECU) when a resistance of approximately 50kΩ is placed between any of the high voltage lines (B+ or B-) and the electronic ground.

For testing the disconnection of the motor for overheat the motor maximum temperature was reconfigured to only 80ºC and a nominal torque test was performed without forced cooling. As result, the controller interrupted the power to the motor just before the 80ºC.

D. *Energy monitoring*

It is important to have a mean of measuring the remaining state of charge (SOC) directly on the motorcycle. Two main distinct methods for estimating batteries SOC are voltage based SOC estimation and current based SOC estimation (coulomb counting).

Voltage based SOC estimation is not very used with lithium cells because of their particular flat voltage characteristic during its discharge.

Current based SOC estimation consists in integrating the discharge current during the use of the battery and subtracting this charge to the know initial charge capacity of the battery for obtaining the remaining charge percentage estimate. On practice, the complication comes with the fact that the useable capacity of a cell is not constant but varies significantly with temperature, the charge/discharge rates, the age of the cell, self-discharge rate, etc.

So for better accuracy and commercial applications several algorithms that are more advanced must be implemented. Such implementation for example consists in the use of lockup tables obtained in laboratory tests that helps the BMS to estimate the usable capacity of the battery.

For this first prototype, a simple implementation based on coulomb counting would suffice using (4) and (5) were I_{bat} is the battery current.

$$UsedAh(t) = \frac{1}{3600}\int_0^t I_{bat}\,dt \;\; [Ah] \tag{4}$$

$$Charge(t) = \frac{(FullBattAh - UsedAh(t))}{FullBattAh} \;\; [\%] \tag{5}$$

In the motorcycle these calculations will be made by a microcontroller and therefore will actually be discrete operations leading (4) to be adapted to (6) which in other words is a discrete integration.

$$UsedAh(t) \approx \frac{1}{3600}\left(\sum_{t=0}^{t} UsedAh(t-1) + I_{bat}\Delta t_{interrupt}\right) \;\; [Ah] \tag{6}$$

An easy way to implement this calculation is to create an interrupt (for example on the ECU) each time the transmit process data object (TPDO) containing the battery current is received from motor controller. Knowing the rate at which the TPDO's are sent it would be easy to obtain the charge via discrete integration since the current value and time steps are known. It is also important that the interrupt rate is fast enough so current peaks are included in this integration.

E. *Cost analysis*

Making the sum of all electrical and electronic components including motor, motor controller, charger, electronic PCBs, batteries, etc a total cost of approximately 9000 euros was obtained. This is high final cost, which would be much reduced by adopting a mass production approach and more self-developed hardware.

In this cost is not included the man-hours of work or additional engineering and equipment costs like prototyping boards, development tools like the USB-to-CAN device or the automated lithium cell tester.

VII. Conclusions

Even though TLM02e motorcycle prototype was not ready for the 2016 competition, it was important to compare other team's competition results with the physical model simulation. In terms of performance, most of the simulation results were relatively close to real results. This gave credibility the chosen parameters and pilot behavior on the model.

On the test bench, all the electronics worked without EMI problems and even it was not possible to extract more power from the motor due to the limited power of the generator, this experience proved useful. The test bench allowed code development, software and hardware debugging and, above all, gaining confidence and knowledge of the various components of the system before its incorporation in the motorcycle, avoiding thus dangerous situations to the pilot and the equipment.

In general, it was concluded that is very important to know at which level of depth each part of a system should be worked on and to distinguish the essential from the accessory. It is also important to start with simple and reliable implementations and only then proceed to implement complex ideas, since considering them at a first approach could endanger the project reliability or turn it infeasible.

A. Future work

Working in an electric vehicle can get very interdisciplinary within the electrical and computer engineering branch. Being the opportunities to improve the current work many, only a small list is referred to here.

-Mounting of the existing electrical system on the motorcycle and test on dynamometer or track.

-Improvement of the data logging system for validation of dynamic simulation results.

-Study the advantage of multiple gear ratios (gear box, continuously variable transmission (CVT)).

-Study of another accumulator implementations as for example conjunction of supercapacitors and batteries.

-Improve the regenerative braking performance.

-Enhance the motor/generator test bench with the possibility of hardware-in-the-loop (HIL) simulation.

-Build a custom motor controller including the power electronics and motor control logic.

-Enhance embedded system reliability by implementing functional safety processes.

-Implement and test more advance methods for SOC estimation on the motorcycle.

Acknowledgment

Considering the initial goals of this thesis, it was impossible to not refer to work of team colleagues. In this way, I would like to mention all the effort and participation of TLMoto team members. Furthermore, I must thank my thesis supervisor and lab technicians for always assuring that I had all the needed tools and materials to the work and sponsors who are making TLM02e electric motorcycle project economically possible.

References

[1] Moto Student, "IV international competition", http://www.motostudent.com/, accessed aug/2016.
[2] MotoStudent, IV international competition - Competition regulations v2.
[3] Play and drive, "motostudent electric", http://www.playanddrive.com/en/prototypes/ motostudent-electric/, accessed aug/2016.
[4] Lennon Patrick Rodgers, "Electric Vehicle Design, Racing and Distance to Empty Algorithms" M.S. thesis, MIT, Cambridge, 2013.
[5] TLMoto, TLm02e - Model15.6, unpublished.
[6] Heinzman, PMS 150, ID 490 Datasheet.
[7] Tony Foale, "Motorcycle handling and chassis design, the art and science", 2002.
[8] Wikipedia, "Energy storage", https://en.wikipedia.org/wiki/Energy_storage, accessed aug/2016.
[9] The Electropaedia, "Battery Knowledge Base", http://www.mpoweruk.com/, accessed aug/2016.
[10] Sevcon, Gen4 - Applications Reference Manual.
[11] Bender, ISOMETER® IR155-3203/IR155-3204, Insulation monitoring device (IMD) for unearthed DC drive systems (IT systems) in electric vehicles.
[12] Linear Technology, LTC6804-1/LTC6804-2 - Multicell Battery Monitors.
[13] Miguel Guedes, "Battery Management System for Formula Student", IST, Lisboa, 2011.